OITS 610
January 1997

Fluctuations of Spatial Patterns as a Measure of Classical Chaos

Zhen Cao and Rudolph C. Hwa

Institute of Theoretical Science and Department of Physics
University of Oregon, Eugene, OR 97403-5203, USA

Abstract

In problems where the temporal evolution of a nonlinear system cannot be followed, a method for studying the fluctuations of spatial patterns has been developed. That method is applied to well-known problems in deterministic chaos (the logistic map and the Lorenz model) to check its effectiveness in characterizing the dynamical behaviors. It is found that the indices μ_q are as useful as the Lyapunov exponents in providing a quantitative measure of chaos.

1 Introduction

An important feature of classical nonlinear systems is that a trajectory traced out by time evolution is well defined, so the distance between nearby trajectories is a meaningful function of time. The Lyapunov exponents that characterize the distance function have therefore been used widely to describe the chaotic behaviors of such systems. Certain quantum systems, however, do not have such a feature. In particular, self-coupled quantum fields such as those in the ϕ^3 theory do not have evolutionary histories that can readily be described by trajectories, since the number of degrees of freedom changes with time. In such problems alternative criteria for chaos beside the use of Lyapunov exponents must be found. A measure useful in the study of QCD parton showers is a set of indices μ_q that characterize the nature of fluctuations of spatial patterns [1]. It is the purpose of this paper to apply that measure to classical nonlinear systems and investigate its usefulness as an alternative criterion for chaos.

In microscopic quantum systems it is often impossible to track the time evolution of their states without disturbing the systems. Instead, it is the final state that can be measured with high accuracy. A prime example of problems of that type is the inelastic collision of elementary particles at very high energy, where many particles are created. The momenta of all charged particles in the final state can be determined precisely in experiments. Thus for each collisional event the momenta of those particles constitute a spatial pattern in momentum space. From event to event those patterns change not only in the magnitudes and directions of the momentum vectors, but also in the total number of such vectors.

The challenge has been in finding an efficient way of characterizing the fluctuation of those patterns in experiments where millions of events are measured. Moreover, it has been of interest to find out whether the notion of chaos has any meaning for such multiparticle production processes.

In order to answer the latter question, i. e., the meaning of chaos for self-reproducing nonclassical systems, it is necessary to apply a chosen measure of fluctuations in such systems to some classical problems for which the criteria for chaos are well known. The issue becomes the following: if a classical chaotic system exhibits certain familiar characteristics in its time evolution, what can be said about the nature of the spatial patterns associated with its trajectories? In finding an answer to this question we shall have accomplished in making two beginnings: on the one hand, we shall gain some insight on whether the concept of chaos can be generalized to include self-reproducing quantum systems, and on the other, a new approach to the study of classical chaos will be opened up. The latter is an unexpected bonus that results from the attempts to deal with the demands and concerns of a very different field of physics.

In order to render this paper self-contained, a review of the measure of fluctuations will be given (in Sec. 2) without the particle physics in which it is originated. The body of this paper is the application of that measure to the logistic map and the Lorenz attractor [2]. We compare the dependences of the Lyapunov exponents λ on the control parameter r with those of the indices μ_q. It is the close correspondence between the two measures for both deterministic systems that supports our view on the usefulness of $\mu_q > 0$ as a criterion for chaos.

2 Entropy Indices μ_q

Consider the problem of describing a system by making many experimental measurements, each of which is called an event. An event consists of a spatial pattern in d-dimensional space. Let F_q be a measure of that pattern to be described below. From event to event F_q can fluctuate. After $\mathcal{N}$ events, a large number, one has a distribution of F_q, which we denote by $P(F_q)$, normalized to 1. By taking the normalized moments of $P(F_q)$, defined by

$$C_{p,q} = \left\langle F_q^p \right\rangle / \left\langle F_q \right\rangle^p \quad , \tag{1}$$

we have a quantification of the fluctuations of the spatial patterns.

Returning to the definition of F_q itself, it is necessary to recognize first that any description of a spatial pattern depends on the resolution used. Let the d-dimensional space (call it phase space, although it can be just the coordinate space, or just the momentum space, or both) be divided into M bins, each having a volume $V_{\rm bin} = \delta^d$. Furthermore, let the intensity of the pattern be discretized at the bin level so that at the ith bin the bin multiplicity

$$n_i = \int_{V_i} \rho\left(\vec{r}\right) d^d r \tag{2}$$

is rounded out to an integer, where $\rho\left(\vec{r}\right)$ is the density at the point $\vec{r}$. For each event F_q is

defined, for any integer $q \geq 2$, by

$$F_q = \frac{1}{M} \sum_{i=1}^{M} n_i \left(n_i - 1\right) \cdots \left(n_i - q + 1\right) / \left(\frac{1}{M} \sum_{i=1}^{M} n_i \right)^q \tag{3}$$

If Q_n denotes the distribution of bin multiplicity n in the M bins, normalized to $\sum_n Q_n = 1$, then F_q can also be written as

$$F_q = \left\langle n^{[q]} \right\rangle_h / \left\langle n \right\rangle_h^q \tag{4}$$

where $n^{[q]} = n!/(n-q)!$ and $\langle \cdots \rangle_h$ is a (horizontal) average over Q_n. By horizontal, we mean averaging over the multiplicity distribution in a given event, to be distinguished from vertical averaging, such as in (1), which is an average over all events.

The virtue of the normalized factorial moments F_q is that they are trivial for statistical fluctuations [3]. Let Q_n be a Poisson transform

$$Q_n = \int_0^\infty \frac{s^n}{n!} e^{-s} D(s) ds \quad , \tag{5}$$

where $D(s)$ may be regarded as some dynamical distribution, whose convolution with the Poisson distribution (of statistical origin) gives rise to the observed Q_n. It is clear that, since

$$\left\langle n^{[q]} \right\rangle_h = \int_0^\infty s^q D(s) ds \quad , \tag{6}$$

trivial dynamics represented by $D(s) = \delta(s - \bar{n})$ results in $F_q = 1$ for all q. Indeed, (6) indicates that the statistical fluctuation is filtered out from the factorial moments, yielding just the simple moments of the dynamical $D(s)$. Thus F_q provides an effective description of the dynamical fluctuations that generate the spatial pattern under study.

Now let us consider the nature of the fluctuations from event to event. First, (1) can be rewritten in the form

$$C_{p,q} = \left\langle \Phi_q^p \right\rangle \quad , \qquad \Phi_q = \frac{F_q}{\langle F_q \rangle} \quad . \tag{7}$$

While much information can be revealed by studying all moments p of $P(F_q)$, it is sufficient for our purpose here to examine only the neighborhood of $p = 1$. It is analogous to studying the information dimension D_1, which is the fractal dimension at order 1 [4]. With the definition

$$\Sigma_q = \left. \frac{d}{dp} C_{p,q} \right|_{p=1} \quad , \tag{8}$$

we have, on the one hand,

$$\Sigma_q = \langle \Phi_q \ln \Phi_q \rangle \quad . \tag{9}$$

On the other hand, if $C_{p,q}$ has a power-law behavior in M,

$$C_{p,q} \propto M^{\psi_q(p)} \quad , \tag{10}$$

which has been referred to as erraticity [5], then we also have

$$\Sigma_q \propto \frac{d}{dp}\psi_q(p)\bigg|_{p=1} \ln M \quad . \tag{11}$$

For brevity we define

$$\mu_q = \frac{d}{dp}\psi_q(p)\bigg|_{p=1} \quad , \tag{12}$$

and refer to them as entropy indices. It then follows that

$$\mu_q = \frac{\partial \Sigma_q}{\partial \ln M} \tag{13}$$

in the scaling region, i. e., where Σ_q exhibits a linear dependence on $\ln M$. It is not difficult to show how μ_q is related to an entropy defined in the event space [1, 4], but that connection is not needed here.

If there is no strict scaling behavior in M, then (10) may have to be generalized to accommodate a possible scaling law in $g(M)$

$$C_{p,q} \propto g(M)^{\psi_q(p)} \quad , \tag{14}$$

where $g(M)$ is some function of M. In such cases Σ_q and μ_q are defined as in (8) and (12), the only difference being that M is replaced by $g(M)$ in (11) and (13). Thus, instead of (11), we would have

$$\Sigma_q(M, r) \propto \mu_q(r) \ln g(M) \quad , \tag{15}$$

where we have introduced a control parameter r, the dependence on which has been assumed implicitly in the foregoing, but will become explicit in the following sections. The factorizable form of (15) suggests that $g(M)$ may be determined from $\Sigma_q(M, r)$ by evaluating it at a particular r_0 so that

$$\Sigma_q(M, r) \propto \beta_q(r) \Sigma_q(M, r_0) \tag{16}$$

where

$$\beta_q(r) = \mu_q(r)/\mu_q(r_0) \tag{17}$$

In this way $\mu_q(r)$ can be determined only up to an overall factor for all r .

We have described above a procedure by which one can take $\mathcal{N}$ events of fluctuating, spatial patterns, and by using (3), (7), (9) and (13) [or (16) and (17)] determine a set of indices μ_q, $q = 2, 3, \cdots$, that can efficiently characterize the nature of the fluctuations. In practice, it is not necessary to examine a large number of μ_q; μ_2 and μ_3 should suffice. In the following sections we shall use μ_2 as a measure to study the properties of the logistic and Lorenz problems and compare its behaviors with those of the Lyapunov exponents λ.

3 The Logistic Map

The simplest and well-understood example of deterministic chaos is the logistic map [2, 6]. We consider this example to illustrate the use of μ_2, since the value of λ for it is well known and can therefore readily provide a comparison with our result on μ_2.

In the 1-dimensional interval $0 < x < 1$, the map is

$$x_{j+1} = r\, x_j\, (1 - x_j) \quad . \tag{18}$$

By repeated iteration one generates a sequence $T(x_0) = \{x_0, x_1, \cdots, x_j, \cdots\}$, starting from a chosen initial point x_0. Every such sequence can be regarded as a trajectory as time evolves, where the time is identified with the number of iterations. The distance d_j between two trajectories T and T' is $\left|x_j - x'_j\right|$ at the jth step. For $r > r_c = 3.5699456\cdots$, but < 4, d_j can grow exponentially for two nearby trajectories with $d_0 = |x_0 - x'_0| = \epsilon$ infinitesimally small. Except for certain narrow intervals between r_c and 4, λ is positive, and the system exhibits chaotic behavior.

The first question to face is how such a behavior in time evolution can be treated from the point of view of spatial patterns, which is what μ_q are designed to describe. Since a trajectory in this case is automatically a collection $T(x_0)$ of discrete points in x, the answer is, of course, obvious. A judicious choice of a subset of $T(x_0)$ is a spatial pattern of interest, and each event corresponds to a particular initial value x_0. To see what subset is appropriate, we show in Fig. 1 a plot of d_j vs j for $r = 3.99$ and for various small values of d_0. The value of λ can be read off from the initial exponential growth, $d_j = d_0 e^{j\lambda}$, to be $\lambda = 0.66$, very close to the analytical value ln2 at $r = 4$. A significant aspect of Fig. 1 is that even for $d_0 = 10^{-12}$ it takes only 40 time steps for d_j to reach $O(1)$, beyond which d_j fluctuates with no apparent order. At smaller values of r, but above r_c, λ would be smaller and it takes longer for d_j to get beyond the exponential growth phase. Two spatial patterns having infinitesimal d_0 would be nearly the same if the corresponding subsets of $T(x_0)$ and $T'(x'_0)$ consist of only the points in the growth phase. To exhibit chaotic behavior it is necessary that $j > \lambda^{-1} \ln d_0^{-1}$, so our subset $S(x_0) \subset T(x_0)$ should consist of points above that value of j. Since we want to study the relationship between λ and μ_2 for all interesting values of r, our choice of points for $S(x_0)$ is as follows

$$S(x_0) = \{x_\Delta, x_{2\Delta}, \cdots, x_{m\Delta}\}_{x_0} \quad , \tag{19}$$

where $\Delta = 100$, and $m = 20$. Each event of that type has a specific x_0, not included in $S(x_0)$. We generate $\mathcal{N} = 10^5$ events whose initial x_0 are all randomly generated within a small interval $(X_0, X_0 + 10^{-5})$ around an arbitrarily chosen value X_0. For the results to be shown below, X_0 is 0.35436. Thus all $\mathcal{N}$ events correspond to initially nearby trajectories, the distances between any two of which diverge after a certain number of steps.

For each of the $\mathcal{N}$ events generated according to the prescription described above, we divide the unit interval into M bins of δ size, count the number of points that fall into each bin, and calculate $F_q(M)$ for that event by use of (3). Then $\Sigma_q(M)$ is determined by performing the appropriate vertical averaging in (9). With focus on $q = 2$, the dependence of $\Sigma_2(M)$ on $\ln M$ is shown in Fig. 2(a) for a few representative values of r. Evidently, there is no linear dependence. We thus use the generalized scaling form expressed in (14) and

consider the plot of (16). That is done in Fig. 2(b), which shows good linear behavior. The value of r_0 is chosen to be 3.9. The slopes $\beta_2(r)$ can be determined from the best fits of all the points for each r, and give, by (17), the values of $\mu_2(r)$ apart from a multiplicative constant.

Figure 3 shows the comparison of λ and μ_2, where the overall normalization of μ_2 in the figure is adjusted to agree with λ at $r = 3.8$. The error bars on the values of μ_2 are due to the deviations from strict straightlines in Fig. 2(b). Clearly, $\mu_2(r)$ agrees very well with $\lambda(r)$ throughout the whole range of r, except that when $\lambda(r) \leq 0, \mu_2(r)$ can only be zero, since it is a nonnegative quantity.

It is by virtue of Fig. 3 that we infer the effectiveness of using the positivity of μ_2 as a criterion for chaos. In fact, μ_q for higher q have the same property, but they are not needed for the simple system under consideration. Thus we conclude that the fluctuations of spatial patterns can be used to reveal the chaotic behavior through the study of μ_q as much as one can learn from the temporal evolution of nearby trajectories.

4 Lorenz Attractor

We now consider another problem to explore the effectiveness of μ_q in a dissipative dynamical system. The prime example of such systems is the Lorenz model, described by the following equations:

$$\begin{aligned} \dot{x} &= -\sigma(x-y) \quad , \\ \dot{y} &= rx - y - xz \quad , \\ \dot{z} &= -bz + xy \quad . \end{aligned} \tag{20}$$

We fix, as with Lorenz [7], $\sigma = 10$ and $b = 8/3$, and vary r as the control parameter. We discretize the time variable and solve (20) by repeated iterations starting from some arbitrary point away from the fixed points. The critical value r_c of the control parameter, above which the trajectory becomes unstable, depends on the size of the time step δt used. It is found that r_c increases slowly when δt is decreased. For computational efficiency we have chosen $\delta t = 10^{-3}$. Figure 4 shows how rapidly the t dependence of the distance function $d(t)$ changes, when r is increased infintesimally from below to above r_c. We determine the value of λ from straightline fits of the rising portions of $\log d(t)$ for every value of r examined. However, because $\log d(t)$ does not rise linearly with t for $r > r_c$ a range of values of λ can be extracted from the fits. We shall indicate the result by shaded bands in $\lambda(r)$.

We use the same technique as described in Sec. 3 to generate a spatial pattern for each event. For $r > r_c$ the trajectory is the familiar Lorenz attractor. Since it is in 3D, we select 70 points spaced 1 time unit apart (i. e. 10^3 time steps of δt), and then make a projection of them to the x-y plane. Figure 5 shows a typical event. A total of 10^4 events are generated, each of which starts out initially at a random point in a small cube of size 10^{-10} on each side, located at the point $x_0 = 0$, $y_0 = 1$, $z_0 = 0$. Since the Lorenz attractor is confined to a finite region of space, which, when projected onto the x-y plane, shows the points mainly along the diagonal of $x \approx y$. We have rotated the coordinates by $\pi/4$ so that the pattern of points is mainly along the new x axis shown in Fig. 5 ($-30 \leq x \leq 30$) with a dispersion in the

expanded new y-axis ($-10 \leq y \leq 10$). This $2D$ rectangular space is divided into M square bins, and the multiplicity n of points in each bin is counted for the computation of F_q in (3) for each event. Using the procedure described in Sec. 2 the quantity $\sum_2$ is determined and plotted against $\log M$ in Fig. 6(a) for various values of r. Scaling is obtained by plotting against $\sum_2(r_0)$, as in Fig. 6(b), where r_0 is chosen to be 28. From the slopes of the lines in the latter figure the indices $\mu_2(r)$ are determined apart from an overall factor, which is fixed by normalizing $\mu_2(r) = \lambda(r)$ at $r = 22.9$.

Figure 7 shows the results of our calculations of both $\lambda(r)$ and $\mu_2(r)$. As mentioned earlier, because of the complicated t dependence of $d(t)$, there is a band of values of λ for each r. We have determined $\lambda(r)$ only for some representative values of r. Given the errors involved, the agreement between $\lambda(r)$ and $\mu_2(r)$ should be regarded as being quite good. The most important point is that they both show stepwise increase at r_c. Thus the utility of the positivity of $\mu_2(r)$ as a criterion for chaos is clearly as effective as that of $\lambda(r)$.

5 Large M Behavior

In the previous two examples we determine the slopes $\beta_2(r)$ from Figs. 2 and 6 and by use of (16); from $\beta_2(r)$ we obtain $\mu_2(r)$ apart from an overall constant. What we want to emphasize here is that the scaling behaviors are for a range of M that is not asymptotically large, i.e., bin size δ is not infinitesimally small. For generic problems in statistical physics and fractal geometry, the extension toward larger values of M is the conventional procedure. However, for problems that we consider here such an extension is inappropriate. To explain that is the aim of this section.

In fractal geometry, for example, one can take the mathematical limit of smaller and smaller scale. The fractal object can always be examined with finer and finer resolution. But in high-energy physics, on the other hand, the number of particles produced in any collisions is finite at finite energy. In the limit $\delta \to 0$ the bin multiplicities can only be 0 and 1, and all $F_q = 0$ for $q \geq 2$. For the logistic and Lorenz problems that we have examined, we have taken a finite number of points (20 and 70 respectively) to display the spatial patterns. Thus the $M \to \infty$ limit would also be inappropriate. Knowing exactly where all the points are in phase space gives too much information and is not what we seek to determine as the measure that can inform us about chaotic behavior.

What can one say about the large M regions above those considered in Figs. 2 and 6, but not large enough to render all $F_q = 0$? We assert that they are of no dynamical interest. For $q = 2$ it is only necessary to examine the M region in which the bins are small enough to contain two or less points in each bin, but not more. Let M_n^e be the number of bins in the eth event with multiplicity n. Then for that event we have

$$F_2 = \frac{1}{M} \sum_j n_j \left(n_j - 1\right) / \left(\frac{N}{M}\right)^2 = 2MM_2^e/N^2 \quad , \tag{21}$$

where N is the total number of points in the event. If $\mathcal{N}_2$ denotes the number of events out of the total $\mathcal{N}$ events in which $M_2 \neq 0$, but $M_n = 0$ for $n \geq 3$, then we get

$$\langle F_2 \rangle = \frac{2M}{\mathcal{N}N^2} \sum_e M_2^e = 2Mr_2 \langle M_2 \rangle / N^2 \quad , \tag{22}$$

where

$$\langle M_2 \rangle = \frac{1}{\mathcal{N}_2} \sum_{e \in \mathcal{N}_2} M_2^e \quad , \tag{23}$$

and $r_2 = \mathcal{N}_2/\mathcal{N}$ is the fraction of events for which $F_2^e \neq 0$, but $F_{q>2}^e = 0$. From (7), (21) and (22) we have

$$\Phi_2^e = M_2^e / r_2 \langle M_2 \rangle \quad , \tag{24}$$

so that from (9) follows

$$\Sigma_2 = \frac{1}{\mathcal{N}_2} \sum_e B_e \ln B_e - \ln r_2 \quad , \tag{25}$$

when $B_e = M_2^e / \langle M_2 \rangle$. In the limit of large M when $M_2^e \to 1$ for nearly all events, then $B_e \to 1$, and

$$\Sigma_2 \sim -\ln r_2 \quad . \tag{26}$$

Now, the probability for a bin in such events to have $n = 2$ is M^{-2}. Since it can be for any of the M bins, we have

$$r_2 \sim M^{-1} \quad . \tag{27}$$

It then follows from (13) that

$$\mu_2 = 1 \tag{28}$$

The same line of reasoning leads also to the result

$$\mu_q = q - 1 \quad . \tag{29}$$

In our numerical computation we have verified this result in that Figs. 2(a) and 6(a) exhibit straightline behavior at large M with unit slope for all values of r. Since only probabilistic arguments have been used to derive the result, it is independent of the structure of the model.

Thus in the search for scaling behavior in problems where N is finite one should not go to the extreme large M region just before all $F_q \to 0$, even though $\sum_2$ exhibits linear dependence on $\ln M$ there. The behavior that is more relevant to the determination of μ_q involves $g(M)$, defined in (14), as the scaling variable, and it is the plots like Figs. 2(b) and 6(b) that yield the more pertinent straightline behaviors.

6 Concluding Remarks

By working with the two examples, the logistic map and the Lorenz attractor, we have demonstrated that the index μ_2 is as good as λ in marking the chaotic regime of the control

parameters. One may wonder why the complicated procedure to determine μ_2 should be considered when the computation of λ is significantly simpler. We reiterate that the rationale for studying spatial patterns is rooted in the desire to examine chaotic behaviors in systems where following the temporal evolution is not possible, or where trajectories are ill defined. Such problems are far more complicated than the simple nonlinear systems considered in deterministic chaos. The complexity of the procedure described in Sec. 2 for the determination of the entropy indices μ_q is commensurate with the complexity of the problems. Applying such a tool to study the logistic map seems to be an overkill. But it has to be done in order to show the significance of the method. It is only when the agreement between μ_2 and λ is established for problems with known behaviors of λ can one claim that $\mu_2 > 0$ is an effective criterion for chaos, whether the system under study is simple or complex.

Now that we have a method for treating the fluctuations of spatial patterns, there seems to be a wide range of problems that could not be studied effectively previously, but are now amenable to analysis by this method. They may range from cracks in dry lake beds to galactic distribution. When there is only one event, like the astrophysical problem on galaxies, one should divide the whole space into many subspaces, each constituting an event, study the multiplicity fluctuations in bins of various sizes in each subspace (event) and then average the fluctuations of those patterns over all subspaces. Even in problems of conventional deterministic chaos, it is not always easy to fine-tune the initial conditions experimentally. Studying the properties of spatial patterns may allow an experimentalist to circumvent the fine-tuning difficulty. It would be very interesting to explore through the study of μ_2 the possible universality among many fields that have hitherto been regarded as totally unrelated.

Acknowledgment

One of us (RCH) would like to thank T. Hwa for helpful discussions. This work was supported, in part, by the U. S. Department of Energy under Grant No. DE-FG03-96ER40972.

References

[1] Z. Cao and R. C. Hwa, Phy. Rev. Lett. **75**, 1268, (1995); Phys. Rev. D **53**, 6608 (1996).

[2] H. G. Schuster, *Deterministic Chaos* (Physik-Verlag, Weinhein, 1984).

[3] A. Białas and R. Peschanski, Nucl. Phys. **B273**, 703 (1986); **B308**, 867 (1988).

[4] H. G. E. Hertschel and I. Procaccia, Physica **8D**, 435 (1983).

[5] R. C. Hwa, Acta Physica Polon. **B27**, 1789 (1996).

[6] P. Collet and J. P. Eckman, *Iterated Maps on the Interval as Dynamical Systems*, (Birkhauser, Boston, 1980).

[7] E. N. Lorenz, J. Atmos. Sci. **20**, 130 (1963).

Figure Caption

Fig. 1 Exponential growth of the distance d_j between two trajectories as the time step j is increased.

Fig. 2 Behaviors of Σ_2 for the logistic map as a function of (a) $\ln M$ and (b) $\Sigma_2(r_0)$ for various values of the control parameter r. The value of r_0 is chosen to be 3.9.

Fig. 3 A comparison of μ_2 with the Lyapunov exponent λ for the logistic map.

Fig. 4 The behaviors of the distance function $d(t)$ for the Lorenz attractor at two values of r close to r_c.

Fig. 5 The spatial pattern of one event for the Lorenz attractor when projected onto the x-y plane and rotated by $\pi/4$.

Fig. 6 Same as for Fig. 2, but for the Lorenz attractor, and with $r_0 = 28$.

Fig. 7 A comparison of μ_2 with the Lyapunov exponent λ for the Lorenz attractor.

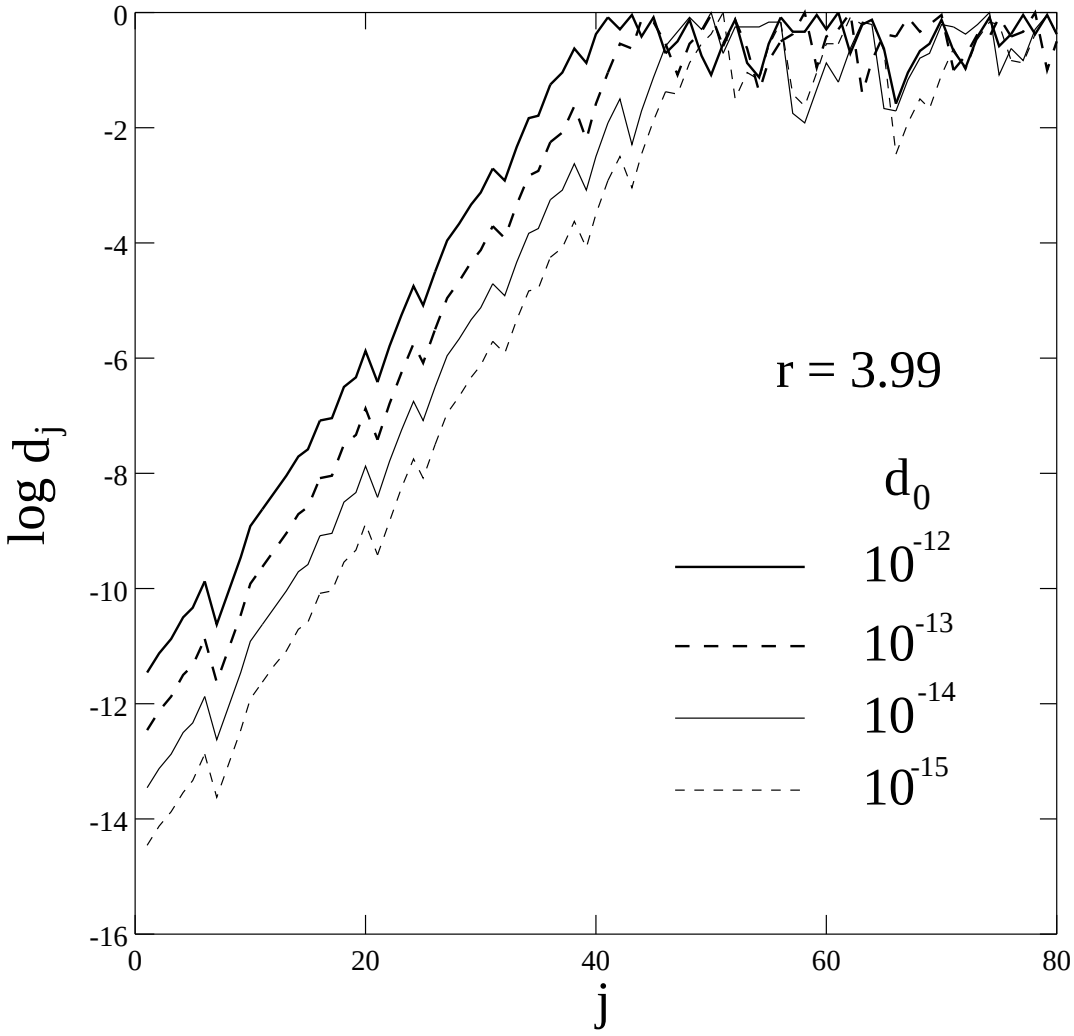
0
-2
-4
-6
-8
-10
-12
-14
-16
0
20
40
60
80
log d_j
j
r = 3.99
d_0
10^{-12}
10^{-13}
10^{-14}
10^{-15}

Fig. 1

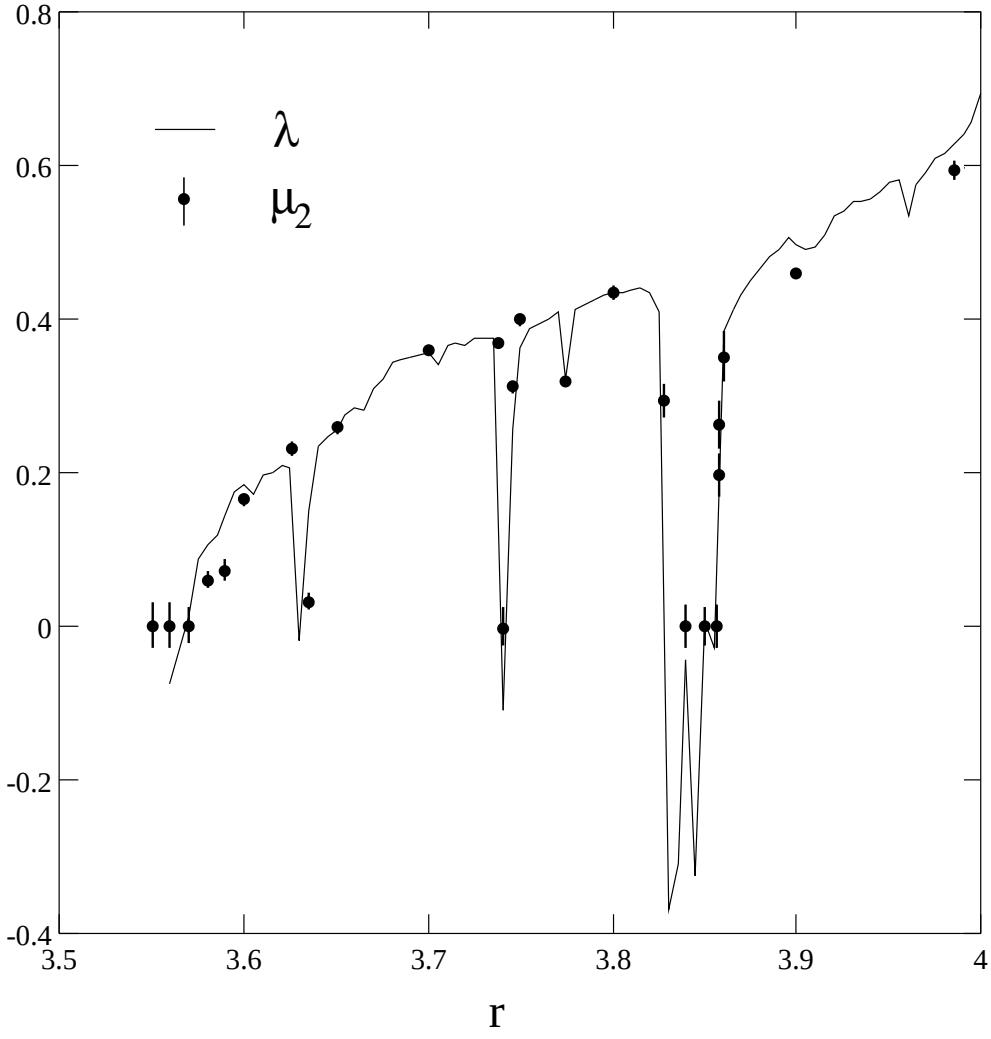

Fig. 3

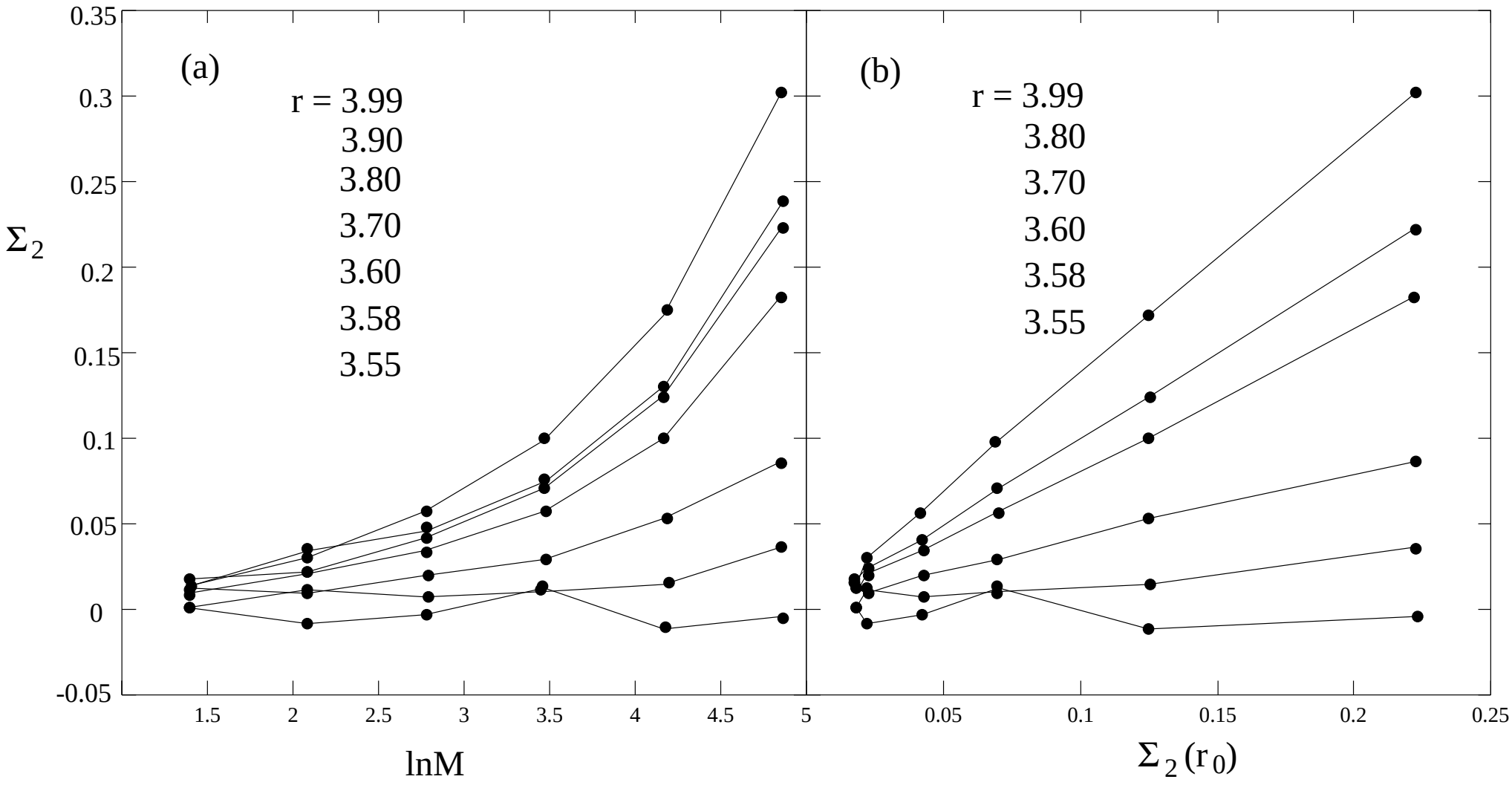
(a)
r = 3.99
3.90
3.80
3.70
3.60
3.58
3.55
Σ_2
lnM
(b)
r = 3.99
3.80
3.70
3.60
3.58
3.55
$\Sigma_2(r_0)$

Fig. 2

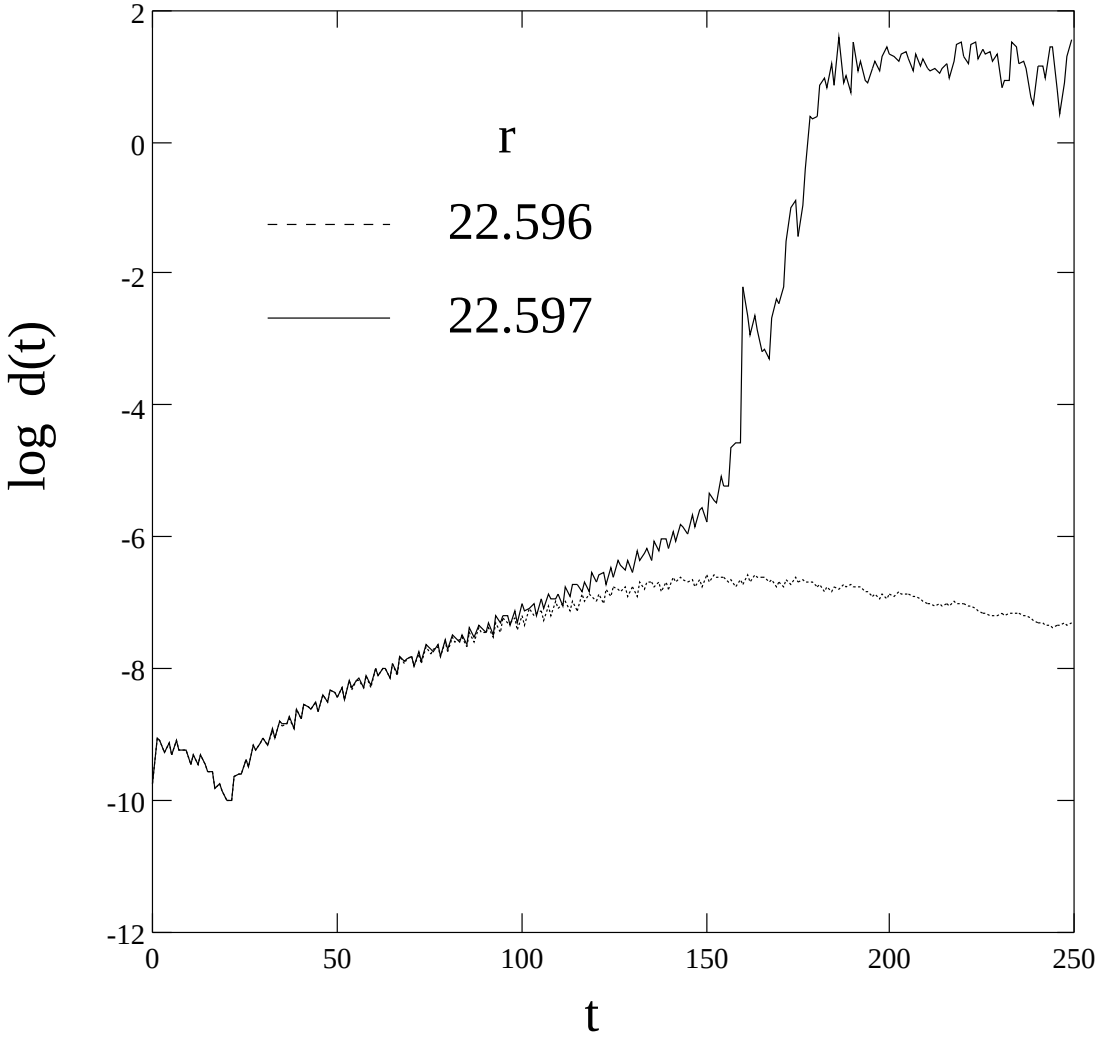

Fig. 4

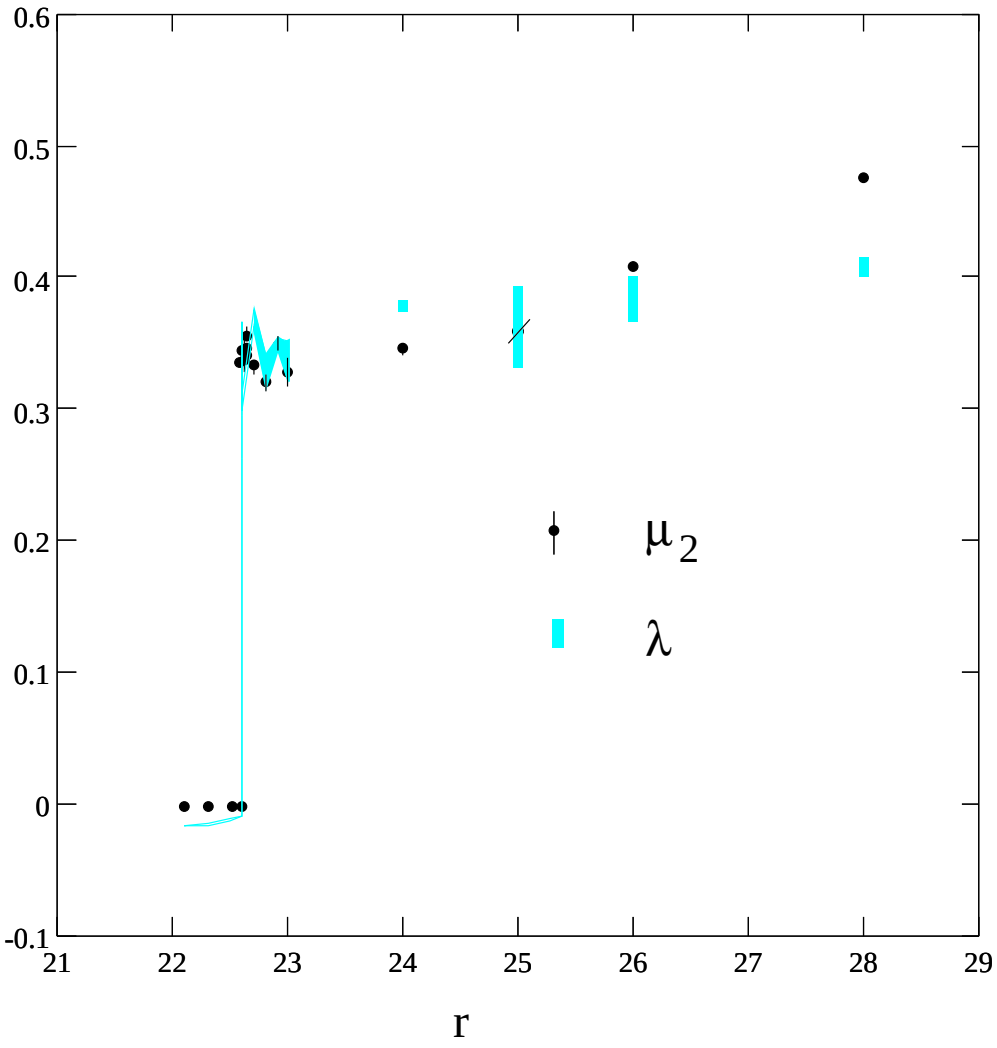

Fig. 7

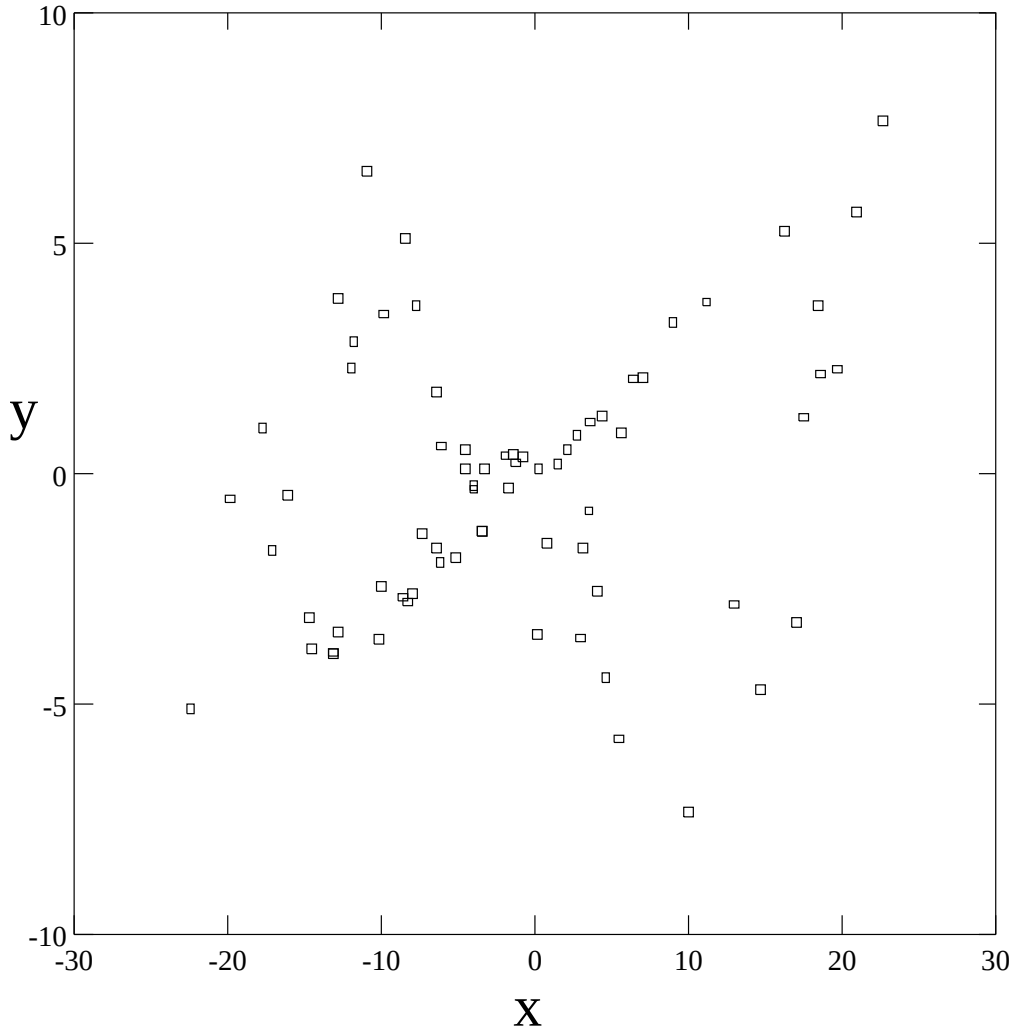

Fig. 5

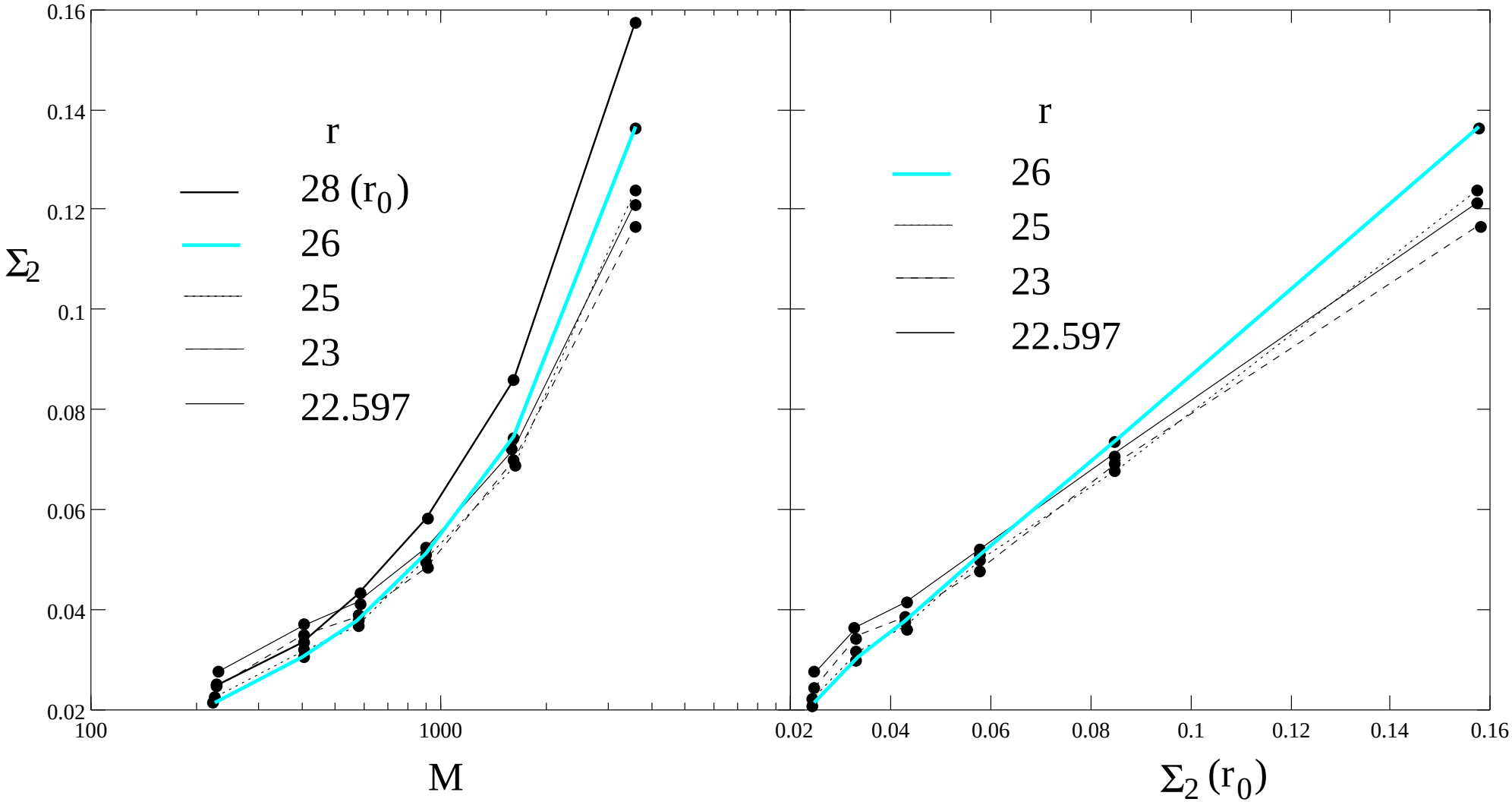
0.16
0.14
0.12
0.1
0.08
0.06
0.04
0.02
Σ_2
r
28 (r_0)
26
25
23
22.597
100
1000
M
0.02
0.04
0.06
0.08
0.1
0.12
0.14
0.16
Σ_2 (r_0)

Fig. 6